

Synthesis and X-ray Crystal Structures of Hexakis(trimethylphosphine)tris- μ -methylene-diruthenium(III) and Its Mono- and Dicationic Derivatives, Hexakis(trimethylphosphine)- μ -methyl-bis- μ -methylene-diruthenium(III) Tetrafluoroborate and Hexakis(trimethylphosphine)bis- μ -methylene-diruthenium(III) Bistetrafluoroborate

Michael B. Hursthouse,* Richard A. Jones, K. M. Abdul Malik, and Geoffrey Wilkinson*

Contribution from the Departments of Chemistry, Imperial College of Science and Technology, London SW7 2AY, England, and Queen Mary College, London E1 4NS, England. Received November 20, 1978

Abstract: The interaction of dimethylmagnesium with the ruthenium(III) trinuclear μ_3 -oxo centered acetate, $[\text{Ru}_3\text{O}(\text{O}_2\text{C-Me})_6(\text{H}_2\text{O})_3](\text{O}_2\text{CMe})$, in the presence of trimethylphosphine yields a unique complex of stoichiometry $(\text{Me}_3\text{P})_3\text{Ru}(\mu\text{-CH}_2)_3\text{-Ru}(\text{PMe}_3)_3$ (**1**), containing three bridging methylene groups. The interaction of this complex with 1 equiv of tetrafluoroboric acid yields a 1+ cationic species, $[(\text{Me}_3\text{P})_3\text{Ru}(\mu\text{-CH}_2)_2(\mu\text{-CH}_3)\text{Ru}(\text{PMe}_3)_3]\text{BF}_4$ (**2**), in which one $\mu\text{-CH}_2$ group is protonated to give a bridging methyl group. With 2 equiv of acid, a 2+ cationic species, $[(\text{Me}_3\text{P})_3\text{Ru}(\mu\text{-CH}_2)_2\text{Ru}(\text{PMe}_3)_3](\text{BF}_4)_2$ (**3**), is formed with loss of methane; this contains only two bridging methylene groups. The corresponding trifluoromethanesulfonate (**4**) has also been obtained. The compounds have been studied by ^1H , ^{31}P , and ^{13}C NMR spectroscopy and their structures have been determined by X-ray crystallography. The compound **1** crystallizes in space group $P2_1/n$ with $a = 22.174$ (5) Å, $b = 9.352$ (2) Å, $c = 16.925$ (4) Å, $\beta = 106.06$ (3)°, and $Z = 4$. The structure was solved by direct methods and refined by least squares to a final R of 0.0292 for 4561 observed data. The overall molecular geometry is that of a confacial bioctahedron. The average Ru-C and Ru-P distances are 2.107 and 2.336 Å, respectively. The Ru-Ru distance of 2.650 (1) Å and acute ($\sim 78^\circ$) Ru-C-Ru angles are consistent with a single Ru-Ru bond as required by the diamagnetism of the compound. Compound **2** crystallizes in space group $P2_1/n$ with $a = 15.216$ (4) Å, $b = 9.930$ (2) Å, $c = 12.579$ (2) Å, $\beta = 109.68$ (2)°, and $Z = 2$. The structure was solved via Patterson and electron density syntheses and refined to an R of 0.049 for 3098 observed data. The dinuclear cation has C_2 symmetry with the bridging CH_2 group sited on the twofold axis and the second CH_2 and the CH_3 groups disordered over the other two equivalent sites. The Ru-C distances are all equal within the limits of experimental error, but the Ru-P bond trans to the unique bridging carbon is longer 2.331 (1) vs. 2.307 (2), 2.314 (2) Å, than the other two. Compound **3** crystallizes in space group $Pbca$ with $a = 12.719$ (2) Å, $b = 16.011$ (3) Å, $c = 17.765$ (2) Å, and $Z = 4$. This structure was also solved by heavy-atom methods and refined to an R of 0.036 for 2370 observed data. The dinuclear cation has $\bar{1}$ symmetry and thus an accurately planar Ru-C-Ru nucleus. Each Ru atom has an approximate square pyramidal coordination with one of the phosphines occupying the axial site. The Ru-P distance to this ligand (2.223 (1) Å) is shorter than those of the others, 2.417, 2.424 (1) Å. The RuC_2Ru unit is symmetrical, with a mean Ru-C distance of 2.071 (5) Å.

Introduction

Compounds containing bridging $-\text{CH}_2-$ (methylene) groups with sp^3 hybridized carbon are so far known only for manganese,¹ rhodium,² osmium,³ and platinum.⁴ Substituted bridge groups $-\text{CR}'\text{R}''$ are also known for manganese,^{1,5} rhenium,⁶ iron,⁷ cobalt,⁸ rhodium,^{2,9} and platinum.⁴ In all cases only single or double bridges have been found. A methylene bridged titanium and aluminum complex has also been reported.¹⁰

We report here full details of the synthesis and X-ray crystal structures of the compound $\text{Ru}_2(\mu\text{-CH}_2)_3(\text{PMe}_3)_6$ (**1**),¹¹ the first compound to have more than one bridging methylene ($-\text{CH}_2-$) group. We also describe the interaction of **1** with tetrafluoroboric acid to form firstly a 1+ cationic species (**2**) in which one of the CH_2 groups is converted to a bridging CH_3 group, and secondly a 2+ ion (**3**) formed by loss of methane. Both compounds have two $\mu\text{-CH}_2$ groups; their structures have also been determined. NMR data for the compounds is collected in Tables I and II and analytical data in Table III.

Results and Discussion

1. Hexakis(trimethylphosphine)tris- μ -methylene-diruthenium(III) (Ru-Ru) (1). This diamagnetic, moderately air sensitive, orange-red crystalline compound was originally isolated in low yield from the reaction between dimethyl-

magnesium and the tetrabridged ruthenium(II,III) acetate chloride $\text{Ru}_2(\text{O}_2\text{CMe})_4\text{Cl}$ in the presence of excess trimethylphosphine. The main product in this reaction is *cis*- $\text{Ru-Me}_2(\text{PMe}_3)_4$.¹² Much higher yields of **1** are obtained if the trinuclear μ_3 oxo-centered ruthenium(III) acetate, $\text{Ru}_3\text{O}(\text{O}_2\text{CMe})_6(\text{H}_2\text{O})_3](\text{O}_2\text{CMe})$,¹³ is used. The identity of the compound **1** was determined by a single-crystal X-ray study and its molecular structure is shown in Figure 1.

The molecule consists of two ruthenium atoms in a slightly distorted octahedral arrangement, joined by three bridging methylene groups. The overall coordination geometry is similar to that in $[\text{Ru}_2\text{Cl}_3(\text{PPhEt}_2)_6]^+$,¹⁴ $\text{Ru}_2\text{Cl}_4(\text{PPhEt}_2)_5$,¹⁵ and $\text{Ru}_2\text{Cl}_5(\text{PBu-n}_3)_4$,¹⁶ all of which contain three bridging chlorine atoms. The Ru-Ru distances in these compounds are rather long (3.115–3.443 Å) and indicate very little or no metal-metal interaction. In the present compound, however, the Ru-Ru distance (2.650 (1) Å) is short [cf. Rh-Rh of 2.665 (1) Å in $\text{Rh}_2(\mu\text{-CH}_2)(\text{CO})_2(\eta\text{-C}_5\text{H}_5)_2$],² and this suggests the presence of a single bond between the two Ru^{III} atoms. This is also required by the observed diamagnetism of the compound. Further, the Ru-C(bridge)-Ru angles [77.7 (1) to 78.1 (3)°] in the compound **1** are narrower than the Ru-Cl(bridge)-Ru angles (84.5–88.3°) in the chloro-bridged compounds mentioned above, but comparable with the Fe-

Table I. ^1H and ^{13}C NMR Data for Methylene-Bridged Ru(III) Compounds

compd	^1H δ values ^a			assignment	$^{13}\text{C}\{^1\text{H}\}$ ^b				
(1) $\text{Ru}_2(\text{CH}_2)_3(\text{PMe}_3)_6$	5.22	bt	(6)	$^3J_{\text{P-H}} = 15$ Hz	$\mu\text{-CH}_2$	131.26 ^c	tt	$^2J_{\text{C-P}} = 45.4, 5.1$ Hz	
	1.42	t ^d	(54)	$J_{\text{P-H}} = 5$ Hz	PMe_3	24.40 ^d	t		$J_{\text{C-P}} = 7.1$ Hz
(2) $[\text{Ru}_2(\text{CH}_3)(\text{CH}_2)_2(\text{PMe}_3)_6](\text{BF}_4)$	7.07 ^{e,f}	t	(4)	$^3J_{\text{P-H}} = 6$ Hz	$\mu\text{-CH}_2$	147.6	bs ^{f,g}	$(-80^\circ\text{C})^h$	
						148.5	bs		
	1.4	bs	(54)		PMe_3	16.0	d		$J_{\text{C-P}} = 26.0$ Hz
						20.8	s ⁱ		
(3) $[\text{Ru}_2(\text{CH}_2(\text{PMe}_3)_6)(\text{BF}_4)_2]$	-5.65	pent	(3)	$^3J_{\text{P-H}} = 2$ Hz	$\mu\text{-CH}_3$	-27.1	bs	(-80°C)	
	8.41	pent	(4)	$^3J_{\text{P-H}} \approx 3.5$ Hz	$\mu\text{-CH}_2$	139.3	s		
	1.3	bs	(54)		PMe_3	16.0	d		$J_{\text{C-P}} = 30.9$ Hz
(4) $[\text{Ru}_2(\text{CH}_2)_2(\text{PMe}_3)_6](\text{SO}_3\text{CF}_3)_2$	7.39	m	(4) ^f		$\mu\text{-CH}_2$				
	1.44	bs	(54)		PMe_3				

^a In C_6D_6 with Me_4Si as internal reference, referenced to Me_4Si (δ 0.0) at 60 MHz and 35°C or at 100 MHz and 28°C . Relative intensity in parentheses, b = broad, pent = pentuplet. ^b In C_6D_6 and internal reference (δ 128.7), referenced to Me_4Si (δ 0.0) at 25.2 MHz at 28°C . Peaks to high frequency of Me_4Si are positive. ^c Partially obscured by solvent resonances. ^d A 1:1:1 triplet. ^e See text. ^f In CD_3NO_2 , with Me_4Si as external reference (^1H). Referenced to Me_4Si (δ 0.0) at δ 57.3 ($^{13}\text{C}\{^1\text{H}\}$). ^g This resonance could be a poorly resolved quartet with $^2J_{\text{P-C}} \approx 3$ Hz. ^h In CD_2Cl_2 referenced to Me_4Si at δ 53.0. ⁱ Relative intensity s:d = 2:1.

Table II. $^{31}\text{P}\{^1\text{H}\}$ NMR Spectra of Ruthenium Compounds

	δ values ^a
(1) $\text{Ru}_2(\text{CH}_2)_3(\text{PMe}_3)_6$	-14.15 s
(2) $[\text{Ru}_2(\text{CH}_3)(\text{CH}_2)_2(\text{PMe}_3)_6](\text{BF}_4)$	-12.0 ^b b
	-8.0 ^b s (65°C)
	3.4 ^c bs
(3) $[\text{Ru}_2(\text{CH}_2)_2(\text{PMe}_3)_6](\text{BF}_4)_2$	-13.0 t $J_{\text{P-P}} = 12.1$ Hz
	-14.1 ^b b

^a In benzene + 10% C_6D_6 , referenced to external 85% H_3PO_4 (δ 0.0) at 40.5 MHz. Peaks to high frequency of reference are positive. ^b In MeNO_2 -10% C_6D_6 . ^c In CH_2Cl_2 -10% C_6D_6 at -80°C .

C(bridge)-Fe angle [$77.6(1)^\circ$] in $\text{Fe}_2(\text{CO})_9$ ¹⁷ which contains a single Fe-Fe bond and also has a confacial bioctahedral geometry.

The molecule possesses an approximate threefold axis of symmetry passing through the Ru-Ru bond, and the relative rotational orientation of the triangular sets of terminal phosphorus atoms differs by 7.23 - 10.72° from that corresponding to perfect eclipsing. Selected torsion angles in the $\text{Ru}_2\text{C}_3\text{P}_6$ core are presented in Figure 2.

The Ru-CH₂ distances [2.103 (6) to 2.112 (4) Å] are all equal within experimental error; similarly the Ru-P distances [2.332 (1) to 2.340 (1) Å] are also equal and comparable with those in $[\text{Ru}_2\text{Cl}_3(\text{Et}_2\text{PhP})_6]^+$.¹⁴ The trimethylphosphine groups have normal bond lengths and angles, and adopt conformations such that the interligand contacts are maximized. The molecular arrangement within the unit cell is shown in Figure 3.

NMR data is consistent with the X-ray diffraction study. The ^1H and $^{13}\text{C}\{^1\text{H}\}$ resonances for the sp^3 -hybridized methylene groups are shifted well downfield, as observed for the other well-characterized bridging -CH₂- compounds.^{1,2} The signals have a triplet structure due to coupling to phosphorus (^1H , δ 5.22, broad triplet, $J = 15$ Hz; $^{13}\text{C}\{^1\text{H}\}$, δ 131.26, triplet of triplets, $J = 45.4, 5.1$ Hz). The trimethylphosphine resonances also have a triplet structure (^1H , δ 1.42, $J = 5.0$ Hz; $^{13}\text{C}\{^1\text{H}\}$, δ 24.4, $J = 7.1$ Hz), while the $^{31}\text{P}\{^1\text{H}\}$ spectrum is a sharp singlet confirming the equivalence of the phosphine groups.

The mechanism of formation of **1** from the oxo-centered ruthenium(III) trimer is obscure, but it seems reasonable to suppose that some type of α -hydrogen transfer from intermediate methyl species is involved, e.g., eq 1, or, less likely,

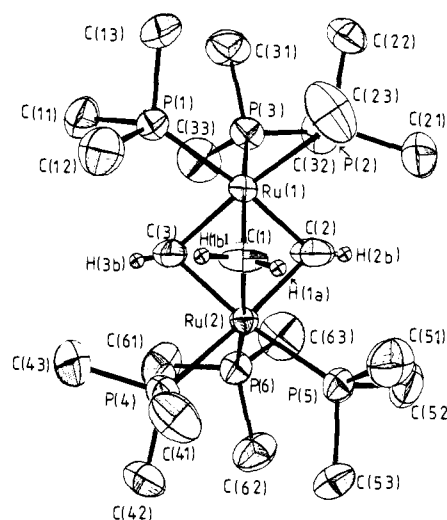
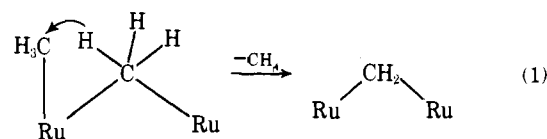
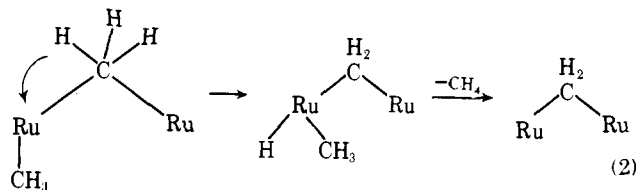


Figure 1. ORTEP³⁰ drawing of the molecule $\text{Ru}_2(\mu\text{-CH}_2)_3(\text{PMe}_3)_6$. Methyl hydrogen atoms are omitted for clarity. Vibrational ellipsoids are drawn at the 50% probability level here and in Figures 4 and 7.



since it would require an oxidative addition to a ruthenium atom already in a 2+ or 3+ state, eq 2. Similar hydrogen



transfers occur in trisium carbonyl cluster compounds³ whereby a $\mu\text{-CH}_3$ group is converted to a $\mu\text{-CH}_2$ group.

2. Hexakis(trimethylphosphine)bis- μ -methylene- μ -methyl-diruthenium(III) Tetrafluoroborate (2). The interaction of **1** with 1 equiv of tetrafluoroboric acid in tetrahydrofuran yields a diamagnetic, air-stable, dark red crystalline compound **2**. Analytical and conductivity data indicate that this compound is a 1:1 tetrafluoroborate salt. NMR spectra show that one of the bridging methylene units in **1** has been protonated

Table III. Analytical Data for Methylene-Bridged Ruthenium Compounds

compd	found, %			calcd, %			Λ_M^b
	C	H	P	C	H	P	
(1) $\text{Ru}_2(\text{CH}_2)_3(\text{PMe}_3)_6^a$	36.5	8.7	27.0	36.0	8.6	26.6	
(2) $[\text{Ru}_2(\text{CH}_3)(\text{CH}_2)_2(\text{PMe}_3)_6]\text{BF}_4$	31.8	7.7	24.0	32.0	7.7	23.6	95 ^c
(3) $[\text{Ru}_2(\text{CH}_2)_2(\text{PMe}_3)_6](\text{BF}_4)_2$	27.9	7.1	23.8	27.9	6.7	21.6	151 ^d
(4) $[\text{Ru}_2(\text{CH}_2)_2(\text{PMe}_3)_6](\text{SO}_3\text{CF}_3)_2$	27.1	6.1	19.6	26.8	5.9	18.9	163 ^e

^a Mol wt cryoscopic in C_6H_6 , found 690 (700). ^b In MeNO_2 at 25 °C, values in $\text{\AA}^{-1} \text{cm}^2 \text{mol}^{-1}$. ^c At $9.0 \times 10^{-4} \text{ M}$. ^d At $7.8 \times 10^{-4} \text{ M}$. ^e At $8.0 \times 10^{-4} \text{ M}$.

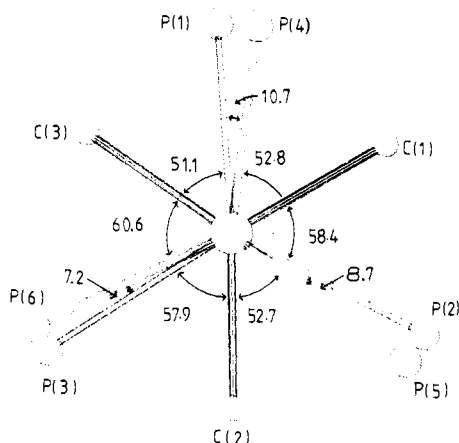


Figure 2. View of the $\text{Ru}_2\text{C}_3\text{P}_6$ central core in the direction of the Ru-Ru axis, showing deviations from exact eclipsing of the P atoms on each metal.

to give a bridging methyl ($\mu\text{-CH}_3$) group. Although as yet rare in transition metal compounds, other examples of bridging methyl groups are known.^{3,18,19,20}

In the ^1H NMR spectrum of **2**, the resonance assigned to the bridging methyl group is shifted greatly upfield ($\delta -5.65$, area 3). The coupling to phosphorus gives a symmetrical pentuplet ($^3J_{\text{P-H}} = 2 \text{ Hz}$). Although this resonance is in the region generally considered to be characteristic of transition metal M-H bonds, there is no evidence for Ru-H bonds from IR spectra in the solid state or in solution. A high upfield shift ($\delta -3.68$) was also reported for the bridging methyl group in $\text{HOs}_3(\text{CO})_{10}(\text{CH}_3)$,³ although the $\mu\text{-CH}_3$ groups of $\text{Re}_3(\text{CH}_3)_9(\text{C}_5\text{H}_5\text{N})_3$ ¹⁸ resonated in the normal region at $\delta -0.7$. The H atoms of the two remaining methylene bridges resonate downfield from the $\mu\text{-CH}_2$ signals in the neutral complex, at $\delta 7.07$, as a slightly distorted quartet ($^3J_{\text{P-H}} = 6 \text{ Hz}$). The ^1H NMR spectrum of **2** prepared using DBF_4 shows a broad high-field resonance with no fine structure at $\delta -5.85$, area 2, which is assigned to $\mu\text{-CH}_2\text{D}$. The resonances of the bridging methylene units are identical with those of the non-deuterated analogue, showing that no proton exchange occurs between the bridging $\text{-CH}_2\text{-}$ and -CH_3 groups. In the $^{13}\text{C}\{^1\text{H}\}$ NMR spectrum the broad resonance to high field of Me_4Si can be assigned to the bridging methyl group ($\delta -27.1$) and again large upfield shifts occur for $\text{HOs}_3(\text{CO})_{10}(\text{CH}_3)$ ³ ($\delta -59.2$) and $\text{Re}_3\text{Me}_9(\text{PEt}_2\text{Ph})_3$ ($\delta -11.83$).²⁰

The methylene carbon atoms give a single slightly broadened resonance, shifted well downfield as in **1** ($\delta 147.6$). At -80°C the resonances are much broader. The $^{31}\text{P}\{^1\text{H}\}$ NMR spectrum consists of a single, sharp resonance at 65°C which becomes very broad at room temperature and at -80°C two considerably sharper resonances are observed (rel intensity 1:2). At elevated temperatures some type of fluxional behavior is evidently occurring. The ^1H NMR resonances also broaden on cooling and are slightly sharper at 50°C .

Although we were hoping that the interaction of **1** with trityl

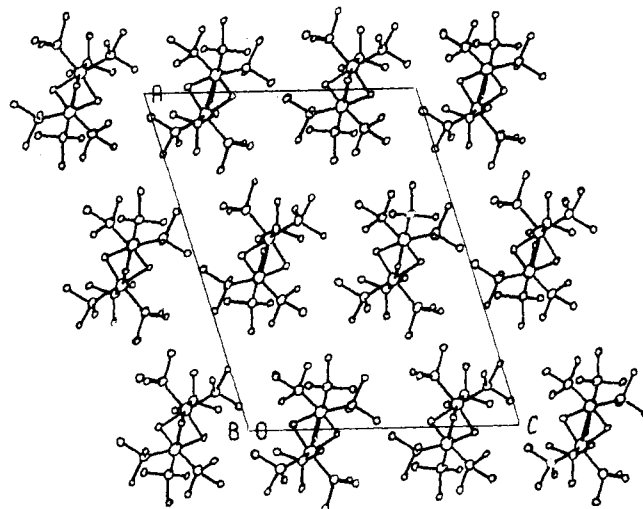
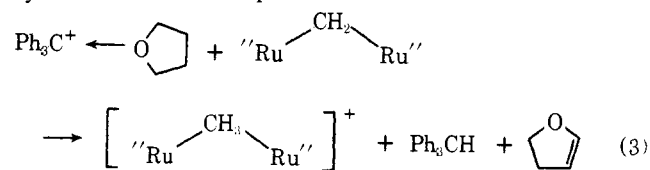


Figure 3. Packing diagram³¹ for $\text{Ru}_2(\mu\text{-CH}_2)_3(\text{PMe}_3)_6$.

tetrafluoroborate would give a compound with a $\mu\text{-CH}$ group, by hydride abstraction, in fact a high yield of **2** was obtained in tetrahydrofuran. Under the conditions used (see Experimental Section) neither **1** nor Ph_3CBF_4 appears to alter in tetrahydrofuran and may be recovered unchanged. It seems most likely that a proton transfer from tetrahydrofuran occurs by a reaction such as eq 3.



The crystal structure of the $1+$ cation as the tetrafluoroborate has been determined by X-ray methods and, although the results are not as clear-cut as one would hope, we feel that they are consistent with the formulation derived from the NMR studies. Routine refinement of this structure was complicated by two features: first, the adoption of rather elongated thermal ellipsoids for some carbon atoms, especially one of the bridge atoms (see Figure 4), and second, our inability to locate hydrogen atoms on these groups. In fact, it was found possible to represent the unique carbon atom on the twofold axis by two half-atoms sited just off the axis (see Experimental Section). We consider that this effect might arise from some orientational disorder and offer the following possible explanation.

We assume that, because of the slightly greater bulk of the methyl over the methylene groups, the dihedral angles between Ru-Me-Ru and Ru-CH₂-Ru planes will be slightly greater than those between the Ru-CH₂-Ru/Ru-CH₂-Ru planes. We then suggest that, for some reason, possibly better packing, the $\mu\text{-methyl}$ group occupies either of the two general positions, along with one of the methylene groups, rather than sits in the unique position on the twofold axis. This situation is represented by Figures 5a and 5b, from which the origin of the split

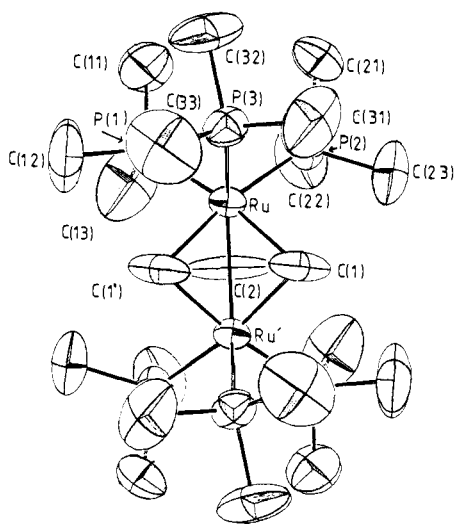


Figure 4. ORTEP³⁰ drawing of the $[\text{Ru}_2(\mu\text{-CH}_2)_2(\mu\text{-CH}_3)(\text{PMe}_3)_6]^+$ cation. Hydrogen atoms are omitted for clarity.

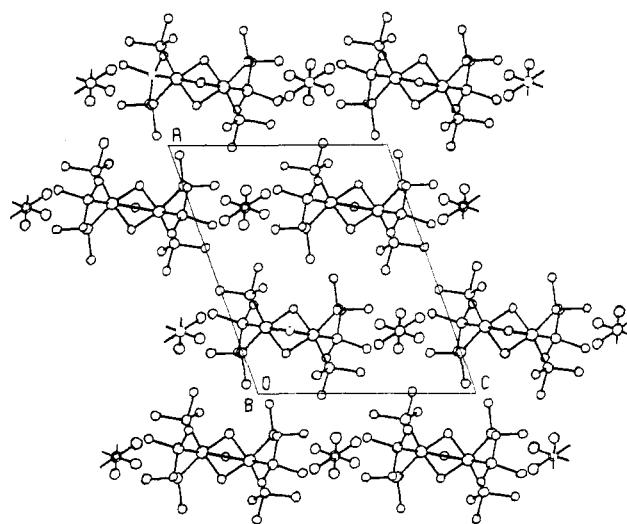


Figure 6. Packing diagram³¹ for $[\text{Ru}_2(\mu\text{-CH}_2)_2(\mu\text{-CH}_3)(\text{PMe}_3)_6]-(\text{BF}_4)$.

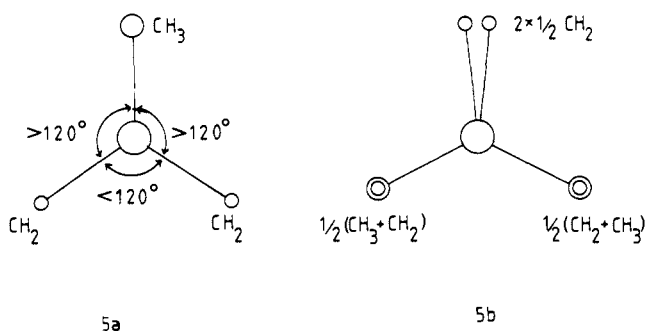
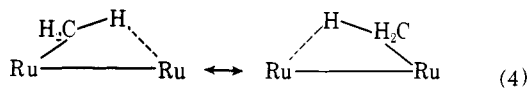


Figure 5. Drawings showing proposed unequal arrangement of the bridging carbon atoms in the $[\text{Ru}_2(\mu\text{-CH}_2)_2(\mu\text{-CH}_3)(\text{PMe}_3)_6]^+$ ion (Figure 5a) and the type of disorder which would give rise to a split C(2) peak on the C_2 axis (Figure 5b). Both views in direction of the Ru–Ru vector.

C(2) peak can be seen. One further reason for adopting this model rather than one in which the $\mu\text{-CH}_3$ group is disordered over all three possible sites arises from perusal of the Ru–P distances. The Ru–P bond trans to the unique bridge atom is longer (2.331 (2) vs. 2.307 (2) and 2.314 (2) Å) than the other two, which are trans to the proposed mixed CH_2/CH_3 sites. This larger value is in fact in excellent agreement with the Ru–P distances in the all-methylene-bridged species **1**. An alternative model, involving an unsymmetrical bridging mode for the CH_3 group of the kind proposed by Shapley,²¹ together with disorder of the type shown in eq 4, is less likely since this



would lead to the thermal ellipsoid for C(2) elongated in a direction perpendicular to that actually observed. The deuteration NMR study (see above) precludes the possibility of proton exchange between CH_3 and CH_2 groups producing a disordered situation.

Because of the uncertainty in our model introduced by the disorder it is impossible to give any detailed discussion of the Ru–C distances except to note that they are all essentially equal and also very similar to those in compound **1**. The overall geometry of the cation is very similar to that of the neutral molecule (**1**) with one important difference. The Ru–Ru distance in **2** is 0.082 Å greater than in **1** [2.732 (1) vs. 2.650 (1) Å] with a concomitant increase of $\sim 4^\circ$ in the Ru–C–Ru angles. Whether this feature is a result of the protonation of one

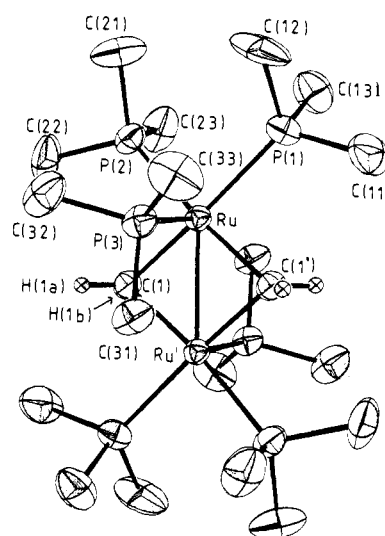


Figure 7. ORTEP³⁰ drawing of the $[\text{Ru}_2(\mu\text{-CH}_2)_2(\text{PMe}_3)_6]^{2+}$ cation. Methyl hydrogen atoms are omitted for clarity.

CH_2 group somehow affecting the strength of the metal–metal bond or of the balancing of the intramolecular–interligand nonbonding interactions is open to debate. We could not find any relevant short contacts in support of the latter idea, however.

The packing of the ions in the unit cell is shown in Figure 6. Some of the fluorine atoms of the BF_4^- ions make short contacts (down to ~ 3.2 Å) with phosphine methyl carbon atoms, but in view of the disorder involving both ions the significance of these is doubtful.

3. Hexakis(trimethylphosphine)bis(μ -methylene)-diruthenium(III) (Ru–Ru) Bistetrafluoroborate (3). The action of 2 equiv or of an excess of tetrafluoroboric or trifluoromethanesulfonic acids on the neutral compound (**1**) yields the orange, diamagnetic, crystalline, air-stable compounds $[(\text{Me}_3\text{P})_3\text{-Ru}(\text{CH}_2)_2\text{Ru}(\text{PMe}_3)_2]\text{X}_2$, X = BF_4^- (**3**) and CF_3SO_3^- (**4**).

The compound **3** may also be obtained by the action of 2 equiv or of an excess of Ph_3CBF_4 in tetrahydrofuran on **1**. If an excess of Ph_3CBF_4 with only a small volume of solvent is used the carbon bridges are lost and an oxygen-bridged complex, $[(\text{Me}_3\text{P})_3\text{Ru}(\mu\text{-O})_2(\mu\text{-OH})\text{Ru}(\text{PMe}_3)_3]\text{BF}_4$ is obtained; this complex will be discussed in a forthcoming paper. This reaction clearly confirms the involvement of tetrahydrofuran in the reactions using Ph_3CBF_4 .

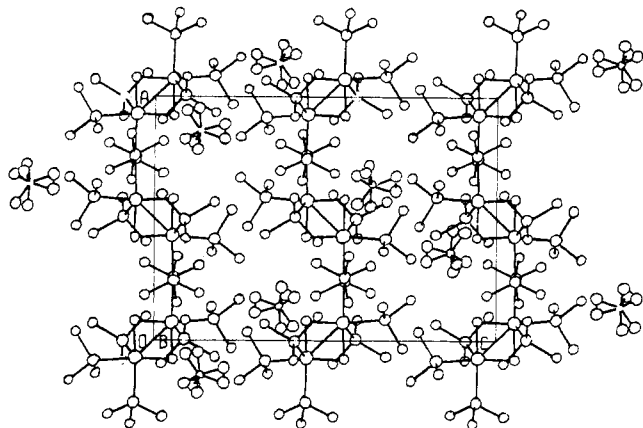


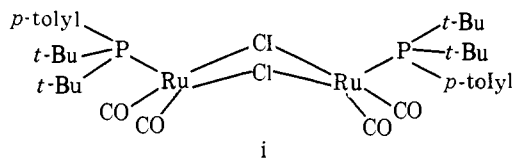
Figure 8. Packing diagram³¹ for $[\text{Ru}_2(\mu\text{-CH}_2)_2(\text{PMe}_3)_6](\text{BF}_4)_2$.

The crystal structure of $[(\text{Me}_3\text{P})_3\text{Ru}(\text{CH}_2)_2\text{Ru}(\text{PMe}_3)_3](\text{BF}_4)_2$ has also been determined.

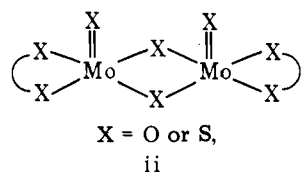
The structure found for the cation is shown in Figure 7. It has a crystallographic inversion center and thus an accurately planar Ru-C-Ru-C nucleus. The Ru-Ru distance [2.641 (1) Å] and the Ru-CH₂-Ru angle (79.2°) are comparable with the corresponding values in **1**, and again indicative of the presence of an Ru-Ru interaction. Each Ru is bonded to two bridging CH₂ and three PMe₃ groups in an approximately square pyramidal environment with one of the phosphines [P(3)] occupying the axial site. The P(1), P(2), C(1), and C(1') atoms forming the pyramid base are planar to within 0.015 Å and the Ru atom is displaced from their mean plane by 0.115 Å toward the axial phosphorus atom.

The Ru-P(3) bond is actually ca. 0.20 Å shorter than the other two [2.223 (1) vs. 2.424 (1) and 2.417 (1) Å] and the two types of bond length represent respectively slight shortening and lengthening compared to values found for the Ru-P bond lengths in compounds **1** and **2**. The two independent Ru-C distances, 2.069 (5) and 2.073 (5) Å, indicate a symmetrical bridge system and are slightly shorter than Ru-C distances in compounds **1** and **2**.

This particular type of dimeric structure, formed from two centrosymmetrically disposed square pyramids, is found quite frequently in copper chemistry.²² However, it contrasts strongly with that found for the complex²³ **i**, which is assigned



a bent Ru-Ru bond, and species of the type **ii**, in which the two



square pyramidal coordination polyhedra are joined so that the two axial sites are *cis*.

One particularly interesting feature of the ion **3**, however, is the blocking of the sixth coordination site on each metal by one of the phosphine methyl groups [C(31)] and the existence of a very short intramolecular Ru---H(31b) contact of 2.30 Å. This could well be a bonding interaction and impart a significant stabilizing effect on the molecule since the two electrons in the CH bond would complete an 18-electron configuration

for ruthenium. However, similar short M---H contacts have been observed,¹² which are almost certainly nonbonding.

The ¹H and ¹³C{¹H} NMR spectra of **3** show no high-field resonances assignable as a bridging methyl. In the ¹H NMR spectrum the bridging methylene groups give a symmetrical pentuplet (δ 8.41, ³J_{P-H} = 3.5 Hz) at a field lower than observed in either **1** or **2**. The ¹³C{¹H} spectrum shows a single slightly broadened resonance for the bridging carbon atoms (δ 139.3) and the ³¹P{¹H} is a single broad peak. The spectra are not temperature dependent. The formation of **3** doubtless occurs by protonation of the bridging methyl group in **2** to give methane, which has been detected by mass spectroscopy.

In a subsequent paper chemical reactions of the three compounds will be discussed.

Experimental Section

Microanalyses were by Butterworth Microanalytical Consultancy Ltd., Pascher (Bonn), and Imperial College Laboratories. NMR spectra were recorded on Perkin-Elmer R12B (¹H); Varian XL-100 (¹H, ¹³C, ³¹P, FT). IR spectra were recorded on Perkin-Elmer P.E. 457, 257. Mass spectra were recorded on a V.G. 7070. Conductivity data was obtained on a Mullard conductivity bridge Type E7566/3 with a matching conductivity cell.

All operations were performed under oxygen-free nitrogen or under vacuum. Tetrahydrofuran and petroleum ether (bp 40–60 °C) were dried over sodium-benzophenone and distilled under nitrogen before use. Methanol was dried over magnesium turnings and distilled under nitrogen. Melting points were determined in sealed capillaries under nitrogen (uncorrected).

Hexakis(trimethylphosphine)tris-μ-methylene-diruthenium(III) (Ru-Ru) (1). Dimethylmagnesium (70.0 cm³ of a 1.1 M diethyl ether solution, 0.077 mol) was slowly added (10 min) to a suspension of $[\text{Ru}_3\text{O}(\text{O}_2\text{CMe})_6(\text{H}_2\text{O})_3](\text{O}_2\text{CMe})$ (5.0 g, 0.00636 mol) in tetrahydrofuran (250 cm³) and trimethylphosphine (5.0 cm³) at -20 °C. The solution was allowed to warm slowly (1 h) and stirred at room temperature (48 h). Methane (by infrared) was evolved. The solution was evaporated under vacuum, the residue extracted with petroleum ether (200 cm³), and the solution filtered. On reduction of the filtrate to ca. 50 cm³ and cooling (-20 °C) dark orange-red prisms were obtained. These were filtered, washed with petroleum ether (2 × 3 cm³) at -78 °C, and dried under vacuum. A further batch of **1** could be obtained by evaporation of the filtrate and also by reextraction of the residue with petroleum ether (2 × 200 cm³), etc. Overall yield was 1.8 g (27%) based on Ru content of $[\text{Ru}_3\text{O}(\text{O}_2\text{CMe})_6(\text{H}_2\text{O})_3](\text{O}_2\text{CMe})$, mp 186–188 °C.

IR (Nujol): 1455 s, 1435 m, 1420 w, 1411 m, 1361 w, 1285 s, 1270 s, 926 s br, 835 m, 715 w, 696 s, 650 s cm⁻¹. In air the compound decomposes in ca. 12 h (solid state) and within seconds in solution.

It is soluble in hydrocarbon solvents, THF, and diethyl ether without decomposition, insoluble in acetone, nitromethane, acetonitrile, and water; it decomposes rapidly in CHCl₃ or CH₂Cl₂. The compound does not react with H₂, CO, or C₂H₄ (1 atm, room temperature) and was recovered unchanged from reactions with *n*-BuLi, MeLi, and Na/Hg in THF. With NO an orange-brown solid is obtained which is insoluble in petroleum ether and toluene, but soluble in CH₂Cl₂; with SO₂ an orange powder is formed. *Note:* Lower yields of **1** resulted if less PMe₃ or Me₂Mg than indicated above is used or when the reaction was stopped before ca. 48 h. **1** could not be obtained in higher yields from the reaction of Ru₂^{II,III}(O₂CMe)₄Cl with Me₂Mg and PMe₃ by variations of the reaction conditions or stoichiometries. Low yields (ca. 5%) of *cis*-RuMe₂(PMe₃)₄ are also obtained from the reaction with $[\text{Ru}_2\text{O}(\text{O}_2\text{CMe})_6(\text{H}_2\text{O})_3](\text{O}_2\text{CMe})$. Other Ru₃ oxo-centered species such as $[\text{Ru}_3\text{O}(\text{O}_2\text{C}i\text{-Bu})_6(\text{Mepy})_3]\text{ClO}_4$ or $[\text{Ru}_3\text{O}(\text{O}_2\text{CMe})_6(\text{P}(\text{OPh})_3)_3]$ were not good starting materials for the preparation of **1**: only very low yields resulted using similar conditions to those described above.

Refluxing *cis*-Ru(PMe₃)₄Me₂¹¹ in toluene (48 h), heating in benzene in a sealed tube for 48 h at 150 °C, or the use of UV irradiation failed to produce **1** despite the formation of homogeneous red solutions in both cases. The dialkyl was recovered in high yield from these reactions.

Hexakis(trimethylphosphine)bis-μ-methylene-μ-methyl-diruthenium(III) (Ru-Ru) Tetrafluoroborate (2). A. Fluoroboric acid (0.4 mL of 43% aqueous solution, 1.9 mmol) in tetrahydrofuran (10 cm³) was

Table IV. Crystal Data and Intensity Measurement Parameters

Parameter or exptl detail	C ₂₁ H ₆₀ P ₆ Ru ₂ (1)	(C ₂₁ H ₆₁ P ₆ Ru ₂)(BF ₄) (2)	(C ₂₀ H ₅₈ P ₆ Ru ₂)(BF ₄) ₂ (3)
<i>a</i> , Å	22.174 (5)	15.216 (4)	12.719 (2)
<i>b</i> , Å	9.352 (2)	9.930 (2)	16.011 (3)
<i>c</i> , Å	16.925 (4)	12.579 (2)	17.765 (2)
α , deg	90	90	90
β , deg	106.06 (3)	109.68 (2)	90
γ , deg	90	90	90
<i>U</i> , Å ³	3372.8	1789.6	3617.9
mol wt or formula wt	700.7	788.5	860.3
<i>D</i> _m , g cm ⁻³	1.36	1.46	1.57
<i>Z</i>	4	2	4
<i>d</i> _c , g cm ⁻³	1.38	1.46	1.58
<i>F</i> ₀₀₀	1456	812	1752
space group	<i>P</i> 2 ₁ / <i>n</i>	<i>P</i> 2/ <i>n</i> (or <i>P</i> _{<i>n</i>})	<i>Pbca</i>
μ (Mo K α), cm ⁻¹	11.3	10.8	10.9
λ (Mo K α), Å	0.710 69	0.710 69	0.710 69
scan parameters <i>A</i> , <i>B</i> , deg	0.8, 0.2	0.8, 0.2 ^a	0.8, 0.2
aperture parameters <i>A</i> , <i>B</i> , mm	4.0, 0.2	4.0, 0.0	4.0, 0.0
reflections measured	$\pm h, k, l$	$\pm h, k, l$	h, k, l
θ _{max} , deg	25	27	27
total number recorded	5921	3870	3935
significance test	<i>F</i> _o > 3 σ (<i>F</i> _o)	<i>F</i> _o > 3 σ (<i>F</i> _o)	<i>F</i> _o > 3 σ (<i>F</i> _o)
reflections remaining	4561	3098	2370
decay during collection	6.5%, linear	none	none

^a The crystal used for data collection for **2** was of lower quality than is usually accepted for accurate work but was the best available. Peak widths were rather variable but these parameters were considered to be adequate.

Table V. Fractional Coordinates (Ru and P $\times 10^5$, C $\times 10^4$) and Anisotropic Thermal Parameters ($\times 10^4$) of the Nonhydrogen Atoms for Ru₂(CH₂)₃(PMe₃)₆ (1)^a

atom	<i>x/a</i>	<i>y/b</i>	<i>z/c</i>	<i>U</i> ₁₁	<i>U</i> ₂₂	<i>U</i> ₃₃	<i>U</i> ₂₃	<i>U</i> ₁₃	<i>U</i> ₁₂
Ru(1)	55 046 (1)	14 699 (3)	78 668 (2)	304 (1)	358 (2)	348 (1)	-11 (1)	61 (1)	-12 (1)
Ru(2)	43 447 (1)	7809 (3)	70 283 (2)	291 (1)	360 (2)	344 (1)	7 (1)	67 (1)	2 (1)
P(1)	61 722 (5)	27 945 (12)	72 957 (6)	484 (5)	547 (6)	452 (5)	-27 (5)	154 (4)	-128 (5)
P(2)	56 984 (5)	27 852 (12)	90 863 (6)	521 (6)	488 (6)	390 (5)	-38 (5)	116 (4)	38 (5)
P(3)	62 438 (5)	-3139 (12)	83 932 (6)	490 (6)	489 (6)	514 (6)	1 (5)	94 (5)	112 (5)
P(4)	38 468 (5)	17 577 (12)	57 462 (6)	488 (5)	533 (6)	386 (5)	48 (5)	67 (4)	37 (5)
P(5)	35 029 (5)	11 857 (12)	75 746 (6)	429 (5)	563 (6)	470 (6)	-11 (5)	169 (4)	72 (5)
P(6)	40 782 (5)	-16 000 (11)	66 719 (7)	498 (6)	395 (5)	549 (6)	-20 (5)	189 (5)	-28 (4)
C(1)	4734 (2)	2828 (5)	7360 (3)	424 (22)	392 (23)	790 (32)	-7 (24)	-22 (21)	6 (19)
C(2)	4842 (3)	214 (9)	8235 (4)	517 (28)	1191 (57)	630 (34)	396 (35)	-96 (24)	364 (31)
C(3)	5187 (2)	495 (7)	6703 (3)	360 (20)	798 (36)	478 (26)	-172 (26)	79 (18)	-76 (21)
C(11)	6559 (3)	1798 (8)	6634 (4)	765 (33)	1091 (48)	716 (35)	-186 (33)	425 (28)	-241 (34)
C(12)	5855 (3)	4268 (7)	6582 (4)	934 (43)	811 (42)	823 (40)	273 (33)	225 (31)	-193 (33)
C(13)	6859 (3)	3748 (7)	7925 (3)	646 (32)	1037 (47)	719 (35)	-137 (30)	240 (25)	-416 (31)
C(21)	5245 (3)	2426 (7)	9813 (3)	758 (33)	1210 (51)	582 (30)	-108 (33)	273 (27)	70 (36)
C(22)	6473 (2)	2826 (7)	9847 (3)	648 (30)	895 (39)	534 (28)	-234 (29)	50 (23)	-85 (29)
C(23)	5574 (4)	4726 (6)	8979 (4)	1488 (61)	532 (32)	702 (38)	-123 (28)	171 (38)	172 (38)
C(31)	7093 (2)	75 (7)	8766 (4)	468 (26)	930 (45)	871 (39)	15 (32)	27 (25)	215 (27)
C(32)	6169 (3)	-1292 (7)	9303 (4)	899 (38)	819 (43)	752 (37)	304 (31)	235 (32)	294 (32)
C(33)	6293 (3)	-1847 (7)	7734 (4)	935 (42)	640 (38)	972 (47)	-104 (32)	235 (35)	301 (31)
C(41)	3506 (3)	3534 (6)	5740 (4)	984 (42)	593 (32)	681 (34)	180 (27)	9 (29)	221 (29)
C(42)	3177 (2)	878 (7)	5017 (3)	590 (29)	999 (43)	503 (27)	-12 (28)	-36 (22)	60 (29)
C(43)	4300 (3)	2076 (8)	5013 (4)	818 (40)	1207 (56)	598 (33)	262 (37)	218 (28)	-10 (37)
C(51)	3484 (3)	2860 (7)	8144 (4)	736 (33)	859 (41)	981 (46)	-338 (35)	320 (32)	111 (33)
C(52)	3383 (3)	-98 (7)	8341 (3)	711 (32)	1052 (45)	721 (35)	200 (33)	412 (27)	70 (33)
C(53)	2682 (2)	1219 (6)	6926 (4)	391 (23)	945 (41)	811 (36)	-32 (30)	199 (23)	60 (25)
C(61)	4365 (3)	-2364 (6)	5853 (4)	959 (43)	703 (38)	1059 (47)	-394 (33)	545 (39)	-168 (32)
C(62)	3259 (3)	-2219 (7)	6313 (4)	653 (31)	729 (36)	1057 (45)	-257 (34)	321 (30)	-259 (28)
C(63)	4359 (3)	-2999 (3)	7449 (4)	1211 (51)	472 (30)	1103 (48)	194 (32)	296 (41)	-9 (34)

^a Estimates of standard deviations are given in parentheses in this and other tables throughout this paper. The anisotropic temperature factor exponent takes the form $-2\pi^2(U_{11}h^2a^{*2} + U_{22}k^2b^{*2} + U_{33}l^2c^{*2} + 2U_{23}klb^{*}c^{*} + 2U_{13}hla^{*}c^{*} + 2U_{12}hka^{*}b^{*})$.

added slowly (2 min) to a solution of **1** (1.36 g, 1.9 mmol) in THF (35 cm³) at room temperature. The mixture was rapidly stirred (0.5 h) and the dark red solid was allowed to settle. This was collected, washed with THF (2 \times 50 cm³) and petroleum ether (50 cm³), and dried under vacuum. This residue was dissolved in methanol (30 cm³), filtered, and evaporated to ca. 10 cm³. The solution was warmed briefly

(50 °C) to ensure complete dissolution, then cooled (-20 °C) to yield dark red crystals which were collected, washed with THF (10 cm³) and petroleum ether (10 cm³), and dried under vacuum, yield 1.4 g (90%), mp 300–320 °C dec.

IR (Nujol): 1455 s, 1445 m, 1435 w, 1370 m, 1310 m, 1290 m, 1278 w, 1060 s br, 1045 s sh, 954 s br, 940 s sh, 855 w, 850 w, 725 m, 715

Table VI. Fractional Coordinates ($\times 10^4$), Isotropic Temperature Factors ($\text{\AA}^2 \times 10^3$), and Bonded Distances ($\text{\AA} \times 10^2$) for the Hydrogen Atoms, with Estimates of Standard Deviations in Parentheses for $\text{Ru}_2(\text{CH}_3)_3(\text{PM}_2)_6$ (**1**)

	<i>x</i>	<i>y</i>	<i>z</i>	U_{iso}	<i>d</i>
H(1a) ^a	4511 (18)	3445 (46)	7618 (23)	55 (12)	94 (5)
H(1b)	4790 (22)	3507 (52)	6944 (31)	84 (16)	98 (5)
H(2a)	4964 (26)	-813 (63)	8305 (40)	103 (21)	100 (6)
H(2b)	4757 (27)	5 (77)	8583 (35)	95 (23)	70 (7)
H(3a)	5326 (19)	-492 (51)	6639 (25)	62 (13)	100 (5)
H(3b)	5166 (27)	917 (64)	6300 (35)	107 (24)	78 (6)
H(11a)	6837 (25)	2375 (58)	6358 (31)	<i>b</i>	102 (6)
H(11b)	6238 (26)	1207 (58)	6299 (35)		95 (5)
H(11c)	6818 (27)	1546 (68)	6885 (36)		66 (5)
H(12a)	5533 (25)	3791 (56)	6069 (33)		106 (5)
H(12b)	6222 (24)	4685 (60)	6403 (33)		102 (6)
H(12c)	5662 (28)	4906 (64)	6829 (37)		90 (7)
H(13a)	7108 (25)	4146 (60)	7630 (33)		92 (6)
H(13b)	6724 (26)	4387 (59)	8257 (35)		93 (6)
H(13c)	7131 (25)	3173 (62)	8350 (35)		96 (5)
H(21a)	4745 (25)	2516 (56)	9546 (31)		108 (5)
H(21b)	5276 (28)	1478 (59)	9953 (37)		92 (6)
H(21c)	5350 (24)	3166 (59)	334 (32)		109 (5)
H(22a)	6770 (26)	3161 (64)	9646 (33)		88 (6)
H(22b)	6605 (26)	1959 (64)	31 (33)		89 (6)
H(22c)	6463 (24)	3452 (57)	344 (33)		103 (6)
H(23a)	5642 (25)	5169 (60)	9527 (33)		99 (6)
H(23b)	5143 (25)	4785 (67)	8794 (35)		92 (5)
H(23c)	5805 (27)	5029 (63)	8617 (36)		95 (7)
H(31a)	7301 (27)	-625 (63)	8958 (35)		81 (6)
H(31b)	7218 (26)	548 (62)	8359 (35)		92 (6)
H(31c)	7101 (5)	804 (61)	9223 (35)		103 (6)
H(32a)	5786 (27)	-1811 (63)	9158 (34)		95 (6)
H(32b)	6424 (25)	-2038 (64)	9472 (33)		89 (6)
H(32c)	6131 (28)	-759 (63)	9688 (34)		84 (6)
H(33a)	6566 (26)	-2373 (62)	8018 (34)		82 (5)
H(33b)	6443 (27)	-1480 (64)	7317 (35)		93 (7)
H(33c)	5897 (25)	-2217 (62)	7495 (33)		93 (5)
H(41a)	3324 (27)	3891 (60)	5256 (36)		87 (6)
H(41b)	3797 (27)	4124 (62)	6121 (36)		95 (5)
H(41c)	3200 (27)	3631 (63)	6052 (35)		97 (7)
H(42a)	2884 (27)	816 (63)	5276 (35)		88 (7)
H(42b)	3016 (26)	1358 (60)	4543 (36)		90 (6)
H(42c)	3273 (25)	-214 (67)	4817 (33)		112 (6)
H(43a)	4537 (27)	2765 (65)	5235 (36)		85 (6)
H(43b)	4043 (25)	2549 (61)	4524 (33)		97 (5)
H(43c)	4418 (28)	1184 (62)	4934 (38)		90 (6)
H(51a)	3471 (29)	3606 (64)	7804 (36)		90 (6)
H(51b)	3842 (26)	2979 (67)	8563 (34)		91 (5)
H(51c)	3079 (25)	2883 (61)	8347 (32)		105 (6)
H(52a)	3732 (27)	-81 (67)	8722 (36)		86 (5)
H(52b)	3021 (26)	172 (62)	8575 (33)		102 (6)
H(52c)	3332 (27)	-1043 (61)	8068 (35)		99 (6)
H(53a)	2425 (27)	1249 (58)	7276 (33)		93 (6)
H(53b)	2571 (26)	361 (62)	6594 (35)		97 (6)
H(53c)	2659 (25)	2118 (61)	6564 (34)		103 (6)
H(61a)	4151 (26)	-3300 (64)	5720 (34)		99 (6)
H(61b)	4829 (26)	-2340 (61)	5948 (33)		100 (6)
H(61c)	4157 (29)	-1774 (68)	5482 (35)		87 (6)
H(62a)	3186 (26)	-3281 (64)	6160 (33)		103 (6)
H(62b)	3040 (26)	-1731 (62)	5747 (34)		105 (5)
H(62c)	3106 (27)	-1977 (66)	6702 (35)		85 (7)
H(63a)	3970 (26)	-2803 (64)	7656 (34)		103 (6)
H(63b)	4176 (25)	-4084 (63)	7127 (33)		117 (6)
H(63c)	4861 (26)	-2924 (63)	7544 (30)		108 (6)

^a H atoms are numbered according to the parent C atom, distinguished by suffixes a, b, or c if more than one is present. ^b One common U_{iso} for all the methyl hydrogen atoms refined to a final value of 0.105 (4) \AA^2 .

m, 670 cm^{-1} , IR in fluorocarbon Voltalef 3S (BDH): 2970 w, 2908 m, 2880 $\text{w} \text{cm}^{-1}$.

B. A solution of trityl tetrafluoroborate (0.23 g, 0.77 mmol) in THF (40 cm^3) was added to a solution of **1** (0.54 g, 0.77 mmol) in THF (40 cm^3) and the solution stirred (1 h). The red powder was collected, washed with THF ($2 \times 30 \text{ cm}^3$) and petroleum ether ($2 \times 30 \text{ cm}^3$), and dried under vacuum, yield 90%.

Note that Ph_3CBF_4 dissolves slowly (0.5 h) in THF giving a pale yellow solution at room temperature from which it can be quantitatively recovered.

The compound is soluble in nitromethane, acetonitrile, acetone, and methanol, although heating in MeNO_2 (60 $^\circ\text{C}$) for several hours results in some decomposition. It is insoluble in hydrocarbons, THF, and diethyl ether and decomposes in CH_2Cl_2 and CHCl_3 after ca. 0.5 h,

Table VII. Interatomic Distances and Angles for Ru₂(CH₂)₃(PMe₃)₆ (I)

A. Bond Lengths (Å)			
Ru(1)–Ru(2)	2.650 (1)	Ru(2)–C(1)	2.112 (4)
Ru(1)–C(1)	2.111 (4)	Ru(2)–C(2)	2.103 (6)
Ru(1)–C(2)	2.105 (7)	Ru(2)–C(3)	2.105 (5)
Ru(1)–C(3)	2.107 (5)	Ru(2)–P(4)	2.332 (1)
Ru(1)–P(1)	2.335 (1)	Ru(2)–P(5)	2.332 (1)
Ru(1)–P(2)	2.338 (1)	Ru(2)–P(6)	2.340 (1)
Ru(1)–P(3)	2.336 (1)		
P(1)–C(11)	1.841 (7)	P(4)–C(41)	1.824 (6)
P(1)–C(12)	1.839 (6)	P(4)–C(42)	1.841 (5)
P(1)–C(13)	1.831 (6)	P(4)–C(43)	1.825 (7)
P(2)–C(21)	1.821 (7)	P(5)–C(51)	1.845 (7)
P(2)–C(22)	1.839 (5)	P(5)–C(52)	1.840 (7)
P(2)–C(23)	1.837 (6)	P(5)–C(53)	1.848 (4)
P(3)–C(31)	1.849 (5)	P(6)–C(61)	1.823 (7)
P(3)–C(32)	1.838 (7)	P(6)–C(62)	1.841 (5)
P(3)–C(33)	1.838 (7)	P(6)–C(63)	1.837 (6)
B. Nonbonded Distances (Å) in the Coordination Polyhedra			
C(1)···C(2)	2.834	C(3)···P(1)	3.032
C(1)···C(3)	2.760	C(3)···P(3)	3.246
C(2)···C(3)	2.910	C(3)···P(4)	3.191
		C(3)···P(6)	3.133
C(1)···P(1)	3.220	P(1)···P(2)	3.471
C(1)···P(2)	3.108	P(1)···P(3)	3.430
C(1)···P(4)	3.059	P(2)···P(3)	3.468
C(1)···P(5)	3.240		
C(2)···P(2)	3.154	P(4)···P(5)	3.428
C(2)···P(3)	3.084	P(4)···P(6)	3.483
C(2)···P(5)	3.010	P(5)···P(6)	3.439
C(2)···P(6)	3.204		
C. Bond Angles (deg)			
Ru(1)–C(1)–Ru(2)	78.1 (3)	Ru(1)–C(3)–Ru(2)	78.0 (2)
Ru(1)–C(2)–Ru(2)	78.1 (3)		
C(2)–Ru(1)–C(1)	84.5 (2)	C(2)–Ru(2)–C(1)	84.5 (3)
C(3)–Ru(1)–C(1)	81.7 (2)	C(3)–Ru(2)–C(1)	81.8 (2)
C(3)–Ru(1)–C(2)	87.4 (2)	C(3)–Ru(2)–C(2)	87.5 (2)
P(1)–Ru(1)–C(1)	92.7 (1)	P(4)–Ru(2)–C(1)	86.9 (1)
P(1)–Ru(1)–C(2)	173.1 (2)	P(4)–Ru(2)–C(2)	171.4 (2)
P(1)–Ru(1)–C(3)	85.9 (1)	P(4)–Ru(2)–C(3)	91.8 (1)
P(2)–Ru(1)–C(1)	88.4 (1)	P(5)–Ru(2)–C(1)	93.5 (1)
P(2)–Ru(1)–C(2)	90.3 (2)	P(5)–Ru(2)–C(2)	85.3 (2)
P(2)–Ru(1)–C(3)	170.1 (1)	P(5)–Ru(2)–C(3)	171.8 (1)
P(2)–Ru(1)–P(1)	95.9 (1)	P(5)–Ru(2)–P(4)	94.6 (1)
P(3)–Ru(1)–C(1)	171.2 (1)	P(6)–Ru(2)–C(1)	170.8 (1)
P(3)–Ru(1)–C(2)	87.8 (2)	P(6)–Ru(2)–C(2)	92.2 (2)
P(3)–Ru(1)–C(3)	93.8 (1)	P(6)–Ru(2)–C(3)	89.5 (2)
P(3)–Ru(1)–P(1)	94.5 (1)	P(6)–Ru(2)–P(4)	96.4 (1)
P(3)–Ru(1)–P(2)	95.8 (1)	P(6)–Ru(2)–P(5)	94.8 (1)
Ru(1)–P(1)–C(11)	116.0 (2)	Ru(2)–P(4)–C(41)	116.8 (2)
Ru(1)–P(1)–C(12)	119.9 (2)	Ru(2)–P(4)–C(42)	122.4 (2)
Ru(1)–P(1)–C(13)	122.6 (2)	Ru(2)–P(4)–C(43)	119.2 (2)
Ru(1)–P(2)–C(21)	119.9 (2)	Ru(2)–P(5)–C(51)	118.7 (2)
Ru(1)–P(2)–C(22)	122.5 (2)	Ru(2)–P(5)–C(52)	117.5 (2)
Ru(1)–P(2)–C(23)	116.5 (2)	Ru(2)–P(5)–C(53)	122.2 (2)
Ru(1)–P(3)–C(31)	122.0 (2)	Ru(2)–P(6)–C(61)	116.9 (2)
Ru(1)–P(3)–C(32)	117.3 (2)	Ru(2)–P(6)–C(62)	122.7 (2)
Ru(1)–P(3)–C(33)	118.6 (2)	Ru(2)–P(6)–C(63)	118.8 (2)
C(11)–P(1)–C(12)	97.9 (3)	C(41)–P(4)–C(42)	98.4 (3)
C(11)–P(1)–C(13)	98.5 (3)	C(41)–P(4)–C(43)	98.8 (3)
C(12)–P(1)–C(13)	97.0 (3)	C(42)–P(4)–C(43)	96.4 (3)
C(21)–P(2)–C(22)	96.5 (3)	C(51)–P(5)–C(52)	99.1 (3)
C(21)–P(2)–C(23)	98.8 (3)	C(51)–P(5)–C(53)	97.7 (3)
C(22)–P(2)–C(23)	97.7 (3)	C(52)–P(5)–C(53)	96.8 (3)
C(31)–P(3)–C(32)	97.6 (3)	C(61)–P(6)–C(62)	98.3 (3)
C(31)–P(3)–C(33)	97.8 (3)	C(61)–P(6)–C(63)	98.3 (3)
C(32)–P(3)–C(33)	98.9 (3)	C(62)–P(6)–C(63)	96.9 (3)

Table VIII. Fractional Coordinates (Ru $\times 10^5$, Others $\times 10^4$) and Anisotropic Thermal Parameters ($\times 10^4$) of the Nonhydrogen Atoms for $[\text{Ru}_2(\text{CH}_3)(\text{CH}_2)_2(\text{PMe}_3)_6](\text{BF}_4) \cdot 2$ ^a

atom	<i>x/a</i>	<i>y/b</i>	<i>c/z</i>	<i>U</i> ₁₁	<i>U</i> ₂₂	<i>U</i> ₃₃	<i>U</i> ₂₃	<i>U</i> ₁₃	<i>U</i> ₁₂
Ru	26 639 (3)	17 633 (4)	14 970 (3)	655 (3)	465 (2)	455 (2)	-19 (2)	223 (2)	-1 (2)
P(1)	1639 (1)	2853 (2)	-43 (2)	649 (9)	879 (11)	854 (11)	103 (9)	141 (8)	66 (8)
P(2)	3965 (1)	2804 (2)	1312 (2)	614 (9)	793 (10)	1082 (13)	-151 (10)	91 (9)	-127 (8)
P(3)	2809 (1)	-135 (2)	478 (1)	756 (9)	625 (8)	773 (9)	-206 (7)	357 (8)	-67 (7)
C(1)	3400 (7)	827 (9)	3046 (5)	1668 (77)	1229 (62)	640 (36)	256 (38)	652 (45)	583 (57)
C(2)	2500 ^b	3356 (9)	2500 ^b	3976 (284)	540 (54)	1319 (101)	0 ^b	1937 (158)	0 ^b
C(11)	1613 (7)	2655 (13)	-1462 (7)	1309 (82)	1879 (97)	829 (52)	451 (66)	-55 (50)	211 (83)
C(12)	392 (7)	2524 (15)	-355 (9)	869 (57)	2019 (116)	1330 (74)	129 (82)	158 (53)	265 (72)
C(13)	1657 (8)	4729 (10)	6 (10)	1488 (86)	903 (58)	1573 (86)	381 (59)	154 (69)	376 (57)
C(21)	4159 (8)	3073 (13)	-18 (9)	1248 (78)	2231 (132)	1349 (82)	287 (77)	609 (67)	-706 (79)
C(22)	4260 (10)	4393 (13)	2005 (16)	1752 (121)	1436 (102)	3741 (210)	-1547 (131)	1026 (135)	-868 (91)
C(23)	5063 (7)	1818 (14)	2109 (11)	737 (54)	2464 (160)	1650 (106)	260 (90)	191 (61)	308 (70)
C(31)	3553 (11)	-1468 (10)	1249 (10)	2408 (148)	1041 (70)	1544 (95)	8 (66)	453 (95)	808 (87)
C(32)	3216 (9)	-87 (11)	-729 (9)	2110 (115)	1320 (80)	1285 (71)	-476 (63)	1100 (80)	-134 (77)
C(33)	1686 (8)	-1005 (12)	-190 (11)	1259 (75)	1589 (96)	2083 (115)	-1156 (91)	806 (79)	-756 (73)
B ^c	2500 ^b	6172 (13)	7500 ^b	1017 (82)	694 (70)	1067 (91)	0 ^b	497 (75)	0 ^b
F(1)	2500 ^b	7422 (16)	7500 ^b	2490 (229)	1061 (118)	2182 (240)	0 ^b	-76 (172)	0 ^b
F(2)	3204 (9)	5351 (12)	7840 (12)	1849 (104)	1485 (87)	1882 (106)	-126 (81)	255 (83)	926 (80)
F(3)	2780 (18)	6577 (22)	6719 (18)	2745 (237)	2319 (222)	1731 (182)	775 (166)	1141 (181)	-815 (208)
F(4)	1964 (21)	6168 (32)	6351 (24)	1617 (201)	1736 (242)	1664 (230)	-636 (192)	-45 (182)	196 (193)
C(2 _{1/2}) ^d	2182 (11)	3324 (9)	2306 (13)	1530 (188)	473 (48)	558 (100)	110 (49)	599 (11)	184 (66)

^a See footnote a, Table V. ^b Parameters held invariant owing to symmetry requirements. ^c Site occupation factors for the atoms in the BF_4^- anion are as follows: B = 0.50, F(1) = 0.32, F(2) = 0.60, F(3) = 0.45, F(4) = 0.31. ^d Half-atom representation for C(2) (in general position).

Table IX. Fractional Coordinates ($\times 10^4$) and Bonded Distances ($\text{\AA} \times 10^2$) of the Hydrogen Atoms for $[\text{Ru}_2(\text{CH}_3)(\text{CH}_2)_2(\text{PMe}_3)_6](\text{BF}_4) \cdot 2$

atom	<i>x/a</i>	<i>y/b</i>	<i>z/c</i>	<i>d</i>
H(11a) ^a	2175	2698	-1437	85
H(11b)	1225	3027	-1995	82
H(11c)	1614	1568	-1603	109
H(12a)	427	2539	228	72
H(12b)	464	1478	-421	105
H(12c)	-22	2884	-981	90
H(22a)	3760	4832	1102	122
H(22b)	4803	4690	2223	83
H(22c)	4005	5040	2246	86

^a See footnote a, Table VI.

although it is stable in CH_2Cl_2 at -80°C for prolonged periods.

It reacts with excess MeLi in THF to give **1** in good yield, although the reaction in Et_2O is very slow (days).

Hexakis(trimethylphosphine)bis- μ -methylene-diruthenium(III)-(Ru-Ru) Bistetrafluoroborate (3) and Trifluoromethanesulfonate (4). A. Fluoroboric acid (0.58 mL, 43% aqueous solution, 2.8 mmol) in THF (10 cm^3) was added to a solution of **1** (1.0 g, 1.4 mmol) in THF (40 cm^3) at room temperature. The mixture was rapidly stirred (3 h). The orange solid was allowed to settle, collected, washed with THF (2 \times 50 cm^3) and petroleum ether (50 cm^3), and dried under vacuum. It was recrystallized from methanol (as for **2**), washed with THF (10 cm^3) and petroleum ether (10 cm^3), and dried under vacuum, yield 1.1 g (80%), mp 240–245 $^\circ\text{C}$.

B. To a solution of **1** (0.6 g, 0.86 mmol) in THF (40 cm^3) was added trityl tetrafluoroborate (0.51 g, 1.7 mmol) in THF (50 cm^3). After stirring for 8 h the orange powder was collected, washed with THF (2 \times 30 cm^3) and petroleum ether (2 \times 30 cm^3), and dried under vacuum, yield 80%.

IR (Nujol): 1445 s, 1425 m, 1365 m, 1315 w, 1309 m, 1291 m, 1288 m, 1280 w, 1090 s, 1050 s br, 1038 s sh, 987 w, 945 s, 854 w, 765 w, 720 m, 686 w, 670 w, 517 w, 445 w, 400 w cm^{-1} . The compound has similar solubility properties to those of **2** but is insoluble in CH_2Cl_2 .

C. The procedure was as in A but using $\text{CF}_3\text{SO}_3\text{H}$. The salt was recrystallized from methanol and dried under vacuum, yield 80%, mp 203–207 $^\circ\text{C}$ dec.

IR (Nujol): 1450 s, 1320 m, 1310 m, 1308 m, 1295 m, 1288 m, 1270

s br, 1214 m, 1145 s, 1035 s, 950 s br, 860 m, 752 w, 723 m, 685 w, 675 m, 639 s, 573 w, 520 cm^{-1} .

X-ray Crystallography. A. Data Collection. For all three compounds crystal suitable for X-ray work were mounted under nitrogen in Lindemann capillaries. The crystal systems and preliminary unit cell parameters were obtained from oscillation and Weissenberg photographs. Space groups were determined by examination of photographs for systematic absences and, in the case of **2**, from successful refinement. Accurate cell parameters and orientation matrices for data collection were determined by least-squares refinement of setting angles for series of reflections ($16^\circ < \theta < 18^\circ$) automatically centered on an Enraf-Nonius CAD4 diffractometer.

The same instrument was used for intensity-data collection. In all three cases graphite-monochromatized Mo $K\alpha$ radiation was used, together with an ω - 2θ scan technique. For each measurement the scan width was determined by the equation $S = A + B \tan \theta$; horizontal aperture settings were determined using a similar relationship. Each reflection was given a fast prescan (speed 0.335 $^\circ$ /s in ω) and only those considered significant ($I_{\text{net}} > 5$ counts for **1**, $I > 3.3\sigma(I)$ for **2** and **3** were rescanned such that the final net intensities satisfied preset conditions ($I > 3000$ counts for **1** and $I > 33\sigma(I)$ for **2** and **3** subject to maximum measuring times of 60 s) unless the desired accuracy had been achieved during the prescan. Two standard reflections were measured about every 1 h during data collection as a check on crystal and instrument stability. Each scan consisted of 96 steps with the first and last 16 forming the left (B_L) and right (B_R) backgrounds and the central 64 the basic net count C . Then the final net structure factor amplitude F_o and its standard deviation ($\sigma(F_o)$) were computed from the expressions

$$F_o = \{[C - 2(B_L + B_R)]L\}^{1/2}$$

$$\sigma(F_o) = \{[C + 4(B_L + B_R)]^{1/2}K\}/2F_o$$

where K is a scale factor incorporating the variable measuring times, the Lp^{-1} factor, and a crystal decay factor where appropriate. For all compounds the crystals were not very well formed and face indexing was very difficult. However, test calculations using simple, idealized morphologies showed that variations in transmission factors were less than 5%. Accordingly absorption corrections were not applied. The low values of the R factors reported later are considered to vindicate this decision. Cell dimensions and other crystal data together with specific details of the data collections are recorded in Table IV.

B. Structure Analyses and Refinement. 1. The positions of the two ruthenium and six phosphorus atoms were obtained from the best E map computed with the automatic direct methods routine in

Table X. Interatomic Distances and Interbond Angles for the Ion $[\text{Ru}_2(\text{CH}_3)(\text{CH}_2)_2(\text{PMe}_3)_6]^+$ in 2^a

A. Bond Lengths (Å)			
Ru–Ru'	2.732 (1) ^b	P(1)–C(11)	1.783 (10)
Ru–C(1)	2.109 (7)	P(1)–C(12)	1.833 (10)
Ru–C(2)	2.090 (7)	P(1)–C(13)	1.864 (10)
Ru–P(1)	2.307 (2)	P(2)–C(21)	1.815 (10)
Ru–P(2)	2.314 (2)	P(2)–C(22)	1.785 (10)
Ru–P(3)	2.331 (1)	P(2)–C(23)	1.905 (10)
		P(3)–C(31)	1.798 (10)
		P(3)–C(3)	1.824 (8)
		P(3)–C(33)	1.846 (9)
B. Nonbonded Distances (Å) in the Coordination Polyhedron			
C(1)⋯C(2)	2.832	C(1)⋯P(2)	3.258
C(1)⋯C(1')	2.617	C(1)⋯P(3)	3.193
P(1)⋯P(2)	3.372	C(1')⋯P(1)	3.234
P(1)⋯P(3)	3.408	C(1')⋯P(3)	3.169
P(2)⋯P(3)	3.387	C(2)⋯P(1)	3.062
		C(2)⋯P(2)	3.122
C. Bond Angles (deg)			
Ru–C(1)–Ru'	80.8 (4)	C(1)–Ru–C(2)	84.8 (2)
Ru–C(2)–Ru'	81.6 (4)	C(1)–Ru–C(1')	76.8 (2)
P(1)–Ru–C(1)	168.9 (2)	P(3)–Ru–C(1)	91.8 (2)
P(1)–Ru–C(1')	94.1 (2)	P(3)–Ru–C(1')	91.0 (2)
P(1)–Ru–C(2)	88.2 (1)	P(3)–Ru–C(2)	175.2 (2)
P(2)–Ru–C(1)	94.8 (3)	P(1)–Ru–P(2)	93.8 (1)
P(2)–Ru–C(1')	107.5 (3)	P(1)–Ru–P(3)	94.6 (1)
P(2)–Ru–C(2)	90.1 (1)	P(2)–Ru–P(3)	93.6 (1)
Ru–P(1)–C(11)	124.8 (4)	C(11)–P(1)–C(12)	95.4 (5)
Ru–P(1)–C(12)	117.0 (4)	C(11)–P(1)–C(13)	98.0 (6)
Ru–P(1)–C(13)	116.3 (3)	C(12)–P(1)–C(13)	100.8 (6)
Ru–P(2)–C(21)	124.7 (3)	C(21)–P(2)–C(22)	103.2 (7)
Ru–P(2)–C(22)	115.4 (5)	C(21)–P(2)–C(23)	100.0 (6)
Ru–P(2)–C(23)	110.3 (4)	C(2)–P(2)–C(23)	99.6 (7)
Ru–P(3)–C(31)	117.3 (4)	C(31)–P(3)–C(32)	98.0 (6)
Ru–P(3)–C(32)	123.9 (3)	C(31)–P(3)–C(33)	102.7 (7)
Ru–P(3)–C(33)	112.6 (3)	C(32)–P(3)–C(33)	98.9 (5)

^a In view of the disorder of the BF_4^- anion individual geometry parameters are not quoted. The range of B–F distances is 1.24–1.40 Å.

^b The primed atom is related to the unprimed one by the twofold axis at $1/4, y, 1/4$.

Table XI. Fractional Coordinates (Ru $\times 10^5$, Others $\times 10^4$) and Anisotropic Thermal Parameters ($\times 10^4$) of the Nonhydrogen Atoms for $[\text{Ru}_2(\text{CH}_2)_2(\text{PMe}_3)_6](\text{BF}_4)_2 \cdot 3^a$

atom	<i>x/a</i>	<i>y/b</i>	<i>z/c</i>	<i>U</i> ₁₁	<i>U</i> ₂₂	<i>U</i> ₃₃	<i>U</i> ₂₃	<i>U</i> ₁₃	<i>U</i> ₁₂
Ru	7255 (3)	5 (3)	5316 (2)	294 (2)	272 (2)	265 (2)	–23 (2)	–9 (2)	10 (2)
P(1)	2569 (1)	385 (1)	571 (1)	352 (7)	455 (8)	491 (7)	–6 (7)	–66 (7)	–41 (6)
P(2)	858 (1)	–655 (1)	1751 (1)	512 (8)	458 (8)	307 (6)	23 (6)	–15 (6)	59 (7)
P(3)	45 (1)	1220 (1)	892 (1)	466 (7)	312 (6)	382 (6)	–86 (6)	–26 (6)	37 (6)
C(1)	–788 (4)	–467 (3)	558 (3)	369 (26)	351 (30)	312 (24)	0 (22)	–4 (23)	–28 (24)
C(11)	3155 (5)	845 (5)	–259 (4)	545 (38)	1073 (61)	821 (46)	436 (45)	–56 (35)	–247 (39)
C(12)	3053 (5)	1066 (5)	1324 (5)	556 (42)	982 (59)	1338 (66)	–373 (50)	–454 (44)	–194 (41)
C(13)	3443 (5)	–502 (4)	678 (4)	508 (36)	698 (46)	892 (49)	25 (38)	4 (33)	203 (34)
C(21)	1653 (6)	–207 (5)	2493 (4)	1076 (60)	938 (57)	622 (41)	9 (38)	–480 (42)	–33 (44)
C(22)	–332 (5)	–865 (5)	2270 (3)	867 (49)	896 (53)	539 (37)	232 (36)	333 (35)	144 (41)
C(23)	1369 (6)	–1723 (4)	1684 (3)	1022 (52)	585 (39)	610 (38)	232 (32)	130 (38)	345 (40)
C(31)	–964 (4)	1527 (3)	228 (3)	655 (39)	446 (31)	440 (29)	–38 (26)	–82 (28)	163 (29)
C(32)	–668 (5)	1287 (4)	1774 (3)	935 (49)	613 (38)	470 (33)	–82 (30)	11 (34)	370 (38)
C(33)	823 (5)	2163 (4)	922 (4)	727 (45)	356 (32)	1058 (53)	–50 (36)	–103 (39)	–50 (31)
B ^b	1404 (10)	1924 (7)	3651 (7)	1001 (83)	869 (74)	1088 (82)	–560 (67)	–550 (72)	436 (69)
F(1)	1869 (5)	1186 (3)	3841 (3)	1631 (52)	884 (34)	1459 (48)	–102 (32)	–259 (39)	263 (36)
F(2)	1132 (14)	1968 (10)	2951 (8)	2591 (184)	1406 (89)	1113 (85)	–311 (66)	–925 (120)	204 (125)
F(3)	575 (14)	2136 (21)	4067 (11)	1204 (125)	2011 (141)	2420 (192)	–766 (117)	160 (122)	482 (113)
F(4)	2172 (13)	2555 (11)	3735 (15)	911 (88)	636 (72)	2465 (297)	–272 (107)	–719 (123)	126 (64)
F(5)	1753 (26)	2392 (15)	4109 (17)	2944 (370)	1517 (195)	2027 (243)	–990 (173)	–896 (253)	135 (197)
F(6)	476 (21)	1602 (35)	3708 (26)	576 (138)	5976 (918)	2329 (380)	–350 (453)	–235 (172)	–981 (299)
F(7)	1751 (27)	2011 (31)	2950 (17)	1362 (254)	2412 (294)	786 (159)	559 (178)	146 (152)	–141 (224)

^a See footnote a, Table V. ^b Site occupation factors for the atoms in the BF_4^- anion are as follows: B = 1.0, F(1) = 1.0, F(2) = 0.75, F(3) = 0.67, F(4) = 0.50, F(5) = 0.50, F(6) = 0.33, F(7) = 0.25.

SHELX.²⁵ Several cycles of isotropic least-squares refinement of these atoms were followed by a difference electron density synthesis from which all the carbon atoms were located. Refinement was continued first with isotropic and then anisotropic thermal parameters for

nonhydrogen atoms. All hydrogen atoms were then located from difference maps and included in the refinement with individual U_{iso} values for the methylene hydrogens and an overall U_{iso} value for methyl hydrogens. Owing to the large number of parameters, the final

Table XII. Fractional Coordinates ($\times 10^4$), Isotropic Temperature Factors ($\text{\AA}^2 \times 10^3$), and Bonded Distances ($\text{\AA} \times 10^2$) of the Hydrogen Atoms for $[\text{Ru}_2(\text{CH}_2)_2(\text{PMe}_3)_6](\text{BF}_4)_2$ (3)

atom	x/a	y/b	z/c	U_{iso}	d
H(1a) ^a	-1293 (34)	-215 (26)	903(25)	27 (12)	97 (5)
H(1b)	-854 (31)	-993 (28)	654(21)	18 (11)	86 (4)
H(11a)	2910	1386	-423	<i>b</i>	97
H(11b)	3816	1216	-27		111
H(11c)	3218	580	-785		103
H(12a)	3584	1437	1136		96
H(12b)	3660	1001	1567		89
H(12c)	2555	1600	1006		120
H(13a)	3457	-894	1092		97
H(13b)	3699	-819	305		90
H(13c)	4180	-38	792		121
H(21a)	1597	417	2545		101
H(21b)	2022	-592	2929		110
H(21c)	2497	-325	2405		110
H(22a)	-340	-1038	2720		85
H(22b)	-707	-408	2517		99
H(22c)	-780	-1406	2006		114
H(23a)	2120	-1875	1414		110
H(23b)	2017	-1777	2213		125
H(23c)	1256	-1980	2242		108
H(31a)	-1437	2036	448		109
H(31b)	-1447	1183	-17		93
H(31c)	-734	1740	-188		87
H(32a)	-907	761	1963		96
H(32b)	-243	1161	2062		77
H(32c)	-940	1835	1762		94
H(33a)	1237	2027	1762		98
H(33b)	227	2634	981		107
H(33c)	1278	2381	633		85

^a See footnote a, Table VI. ^b U_{iso} for all methyl hydrogens fixed at 0.05 \AA^2 .

stages of the refinement were carried out in two blocks with the overall scale factor and the three CH_2 groups being refined in all cycles. The weighting scheme $w = 1/[\sigma^2(F_o) + 0.0005F_o^2]$ was applied and this gave flat analyses of variance. The refinement converged at $R_1 = 0.0292$ and $R_2 = 0.0355$ where R_1 and R_2 are given by

$$R_1 = \sum((F_o) - (F_c))/\sum(F_o)$$

$$R_2 = [\sum w(|F_o - F_c|)^2/\sum w(F_o)^2]^{1/2}$$

A final difference map revealed no peaks or troughs of any significance. Fractional coordinates and anisotropic thermal parameters for nonhydrogen atoms, coordinates and isotropic parameters for hydrogen atoms, and bond lengths and angles are given in Tables V, VI, and VII, respectively.

2. The structure was solved and refined on the basis of the space group $P2_1/n$. With $Z = 2$, the dinuclear molecule is required to possess a crystallographic twofold axis passing through the midpoint of the Ru-Ru bond. This was confirmed by a three-dimensional Patterson map from which the position of the unique ruthenium atom was obtained. Following isotropic refinement of the Ru parameters a difference electron-density map revealed the positions of the three unique phosphorus atoms. These four atoms were refined isotropically ($R_1 = 0.18$) and a further difference map revealed the positions of all carbon atoms, the boron atom (on the C_2 axis), and a number of possible fluorine atom positions which indicated that the BF_4 ion was orientationally disordered. In the course of the refinement it was found necessary to use four positions, with fractional occupancies, for the two independent fluorine atoms.

Following refinement with anisotropic thermal parameters for the Ru, P, C, B, and F atoms, 9 of the 31 independent hydrogen atoms in the structure were located in difference maps. Surprisingly, these hydrogen atoms belonged to phosphine methyl groups; no really satisfactory peaks were found which could be considered as hydrogen atoms attached to any of the bridging groups or the other phosphine methyl groups. Our inability to locate hydrogen atoms on the bridging groups was to some extent understandable after we had examined the results of the refinement in more detail. The temperature factor coefficients for many of the carbon atoms indicated considerable thermal motion or, more likely, a small amount of orientational dis-

Table XIII. Interatomic Distances and Interbond Angles for $[\text{Ru}_2(\text{CH}_2)_2(\text{PMe}_3)_6]^{2+}$ Ion in 3^a

A. Bond Lengths (\AA)			
Ru-Ru'	2.641 (1) ^b	P(1)-C(11)	1.808 (6)
Ru-C(1)	2.069 (5)	P(1)-C(12)	1.832 (7)
Ru-C(1')	2.073 (5)	P(1)-C(13)	1.814 (7)
Ru-P(1)	2.424 (1)	P(2)-C(21)	1.809 (6)
Ru-P(2)	2.417 (1)	P(2)-C(22)	1.804 (6)
Ru-P(3)	2.223 (1)	P(2)-C(23)	1.834 (6)
Ru-H(31b')	2.301	P(3)-C(31)	1.811 (5)
		P(3)-C(32)	1.813 (6)
		P(3)-C(33)	1.806 (6)
B. Nonbonded Distances (\AA) in the Coordination Polyhedron			
C(1)...C(1')	3.191	C(1)...P(3)	2.961
C(1)...P(2)	2.995	C(1')...P(3)	2.997
C(1')...P(1)	3.028	P(1)...P(3)	3.524
P(1)...P(2)	3.452	P(2)...P(3)	3.523
C. Bond Angles (deg)			
Ru-C(1)-Ru'	79.2 (2)	C(1)-Ru-C(1')	100.8 (3)
Ru'-Ru-P(3)	86.5 (1)	C(1)-Ru-P(2)	83.4 (1)
C(1)-Ru-P(3)	87.2 (2)	C(1')-Ru-P(1)	84.2 (1)
C(1')-Ru-P(3)	88.4 (2)	P(1)-Ru-P(2)	91.0 (1)
P(1)-Ru-P(3)	98.5 (1)	C(1)-Ru-P(1)	172.5 (2)
P(2)-Ru-P(3)	98.7 (1)	C(1')-Ru-P(2)	172.0 (2)
Ru-P(1)-C(11)	118.5 (2)	C(11)-P(1)-C(12)	102.4 (4)
Ru-P(1)-C(12)	119.7 (3)	C(11)-P(1)-C(13)	98.7 (3)
Ru-P(1)-C(13)	113.5 (2)	C(12)-P(1)-C(13)	100.6 (3)
Ru-P(2)-C(21)	121.2 (3)	C(21)-P(2)-C(21)	99.8 (4)
Ru-P(2)-C(22)	118.8 (2)	C(21)-P(2)-C(22)	102.6 (3)
Ru-P(2)-C(23)	112.0 (2)	C(22)-P(2)-C(23)	99.0 (3)
Ru-P(3)-C(31)	109.0 (2)	C(31)-P(3)-C(32)	101.0 (3)
Ru-P(3)-C(32)	119.7 (2)	C(31)-P(3)-C(33)	100.4 (3)
Ru-P(3)-C(33)	121.8 (2)	C(32)-P(3)-C(33)	101.5 (3)

^a B-F distances in the disordered anions lie in the range 1.19-1.41 \AA . ^b The primed atom is related to the unprimed one by the center of symmetry at 0,0,0.

order about the Ru–Ru bond. In fact the thermal ellipsoid for atom C(2) on the twofold axis was so elongated in the a^* direction ($U_{11} = 0.39 \text{ \AA}^2$) that we investigated the possibility of representing this atom by two separated half-atoms just off the C_2 axis. This worked quite well, with the anisotropic thermal parameters for the half-atom refining to values shown in Table VIII but with the R values as a whole slightly higher ($R_1 = 0.0494$, $R_2 = 0.0723$) than for the initial, normal refinement ($R_1 = 0.0489$, $R_2 = 0.708$). While this simple treatment can by no means be considered as a final model, we feel that it can be used as a pointer to the probable situation. However, in view of the limited quality of the data, we did not consider it worthwhile to explore further the split atom model.²⁶ For the simple, single-atom model in which the nine hydrogen atoms found on difference maps were included in F_c calculations with a common U_{iso} of 0.05 \AA^2 , the final R_1 and R_2 values were 0.0489 and 0.0708, respectively. The weighting scheme used was $w = 1/[\sigma^2(F_o) + 0.0003(F_o)^2]$ and this gave acceptable agreement analyses. A final difference map had no peak $>0.7 \text{ e \AA}^{-3}$. The final atomic parameters and bond lengths and angles are given in Tables VIII–X.

3. The position of the unique Ru atom was determined from a three-dimensional Patterson map which suggested a centrosymmetric dinuclear molecule with an Ru–Ru distance of ca. 2.65 Å. Other nonhydrogen atoms were located from successive difference maps. The BF_3 ion was again found to be disordered and the four fluorine atoms were represented by seven positions with fractional occupancies (which were refined). All hydrogen atoms were located on difference maps but only the two CH_2 hydrogens were allowed to refine freely with isotropic temperature factors. Methyl hydrogens were not refined but included in F_c calculations with a fixed common U_{iso} of 0.05 \AA^2 . The refinement, with anisotropic thermal parameters for all nonhydrogen atoms, converged at $R_1 = 0.037$ and $R_2 = 0.048$. The weighting scheme $w = 1/[\sigma^2(F_o) + 0.0003(F_o)^2]$ was used to give flat analyses of variance. A final difference synthesis revealed no region of electron density greater than 0.5 e \AA^{-3} . Atomic parameters and bond lengths and angles are given in Tables XI–XIII.

For all structure analyses, atomic scattering factors for neutral atoms were taken from ref 27 (Ru, P, F, C, B) and 28 (H), with those for the heavier elements modified for anomalous dispersion using $\Delta f'$ and $\Delta f''$ values taken from ref 29. All computations were made on the Queen Mary College ICI 1904S and University of London CDC 7600 computers.

Acknowledgments. We thank the Science Research Council for a studentship (R.A.J.) and a fellowship (K.M.A.M.), and, together with the Royal Society, for assistance in the purchase of the diffractometer, and Johnson, Matthey Ltd, for the loan of ruthenium.

Supplementary Material Available: Observed and calculated structure factors for $\text{Ru}_2(\text{CH}_2)_3(\text{PMe}_3)_6$, $\text{Ru}_2(\text{CH}_2)_2(\text{PMe}_3)_6 \cdot 2\text{BF}_4$, and $\text{Ru}_2(\text{CH}_3)(\text{CH}_2)_2(\text{PMe}_3)_6 \cdot \text{BF}_4$ (23 pages). Ordering information is given on any current masthead page.

References and Notes

- W. A. Herrmann, B. Reiter, and H. Biersack, *J. Organomet. Chem.*, **97**, 245 (1975).
- W. A. Herrmann, C. Krüger, R. Goddard, and I. Bernal, *J. Organomet. Chem.*, **140**, 73 (1977); *Angew. Chem., Int. Ed. Engl.*, **16**, 334 (1977).
- R. B. Calvert and J. R. Shapley, *J. Am. Chem. Soc.*, **100**, 6544 (1978).
- M. P. Brown, J. R. Fisher, S. J. Franklin, R. J. Puddephat, and K. R. Seddon, *J. Chem. Soc., Chem. Commun.*, 749 (1978).
- A. B. Antonova, N. E. Kolobova, P. V. Petrovsky, B. V. Lobshin, and N. S. Obezyuk, *J. Organomet. Chem.*, **137**, 55 (1977).
- N. E. Kolobova, A. B. Antonova, O. M. Khitrova, M. Yu Antipin, and Yu T. Struchkov, *J. Organomet. Chem.*, **137**, 69 (1977); E. O. Fischer, T. L. Lindner, H. Fischer, G. Hüttner, P. Friedrich, and F. R. Kreissl, *Z. Naturforsch. B*, **32**, 648 (1977).
- E. O. Fischer, V. Klener, and R. D. Fischer, *J. Organomet. Chem.*, **16**, P60 (1969); O. S. Mills and A. D. Redhouse, *J. Chem. Soc. A*, 1282 (1968).
- W. A. Herrmann, *Chem. Ber.*, **111**, 1077 (1978); B. L. Booth, R. N. Hazeldine, P. R. Mitchell, and J. J. Cox, *Chem. Commun.*, 529 (1967); J. Cooke, W. R. Cullen, M. Green, and F. G. A. Stone, *ibid.*, 170 (1968); *J. Chem. Soc. A*, 1872 (1969).
- P. Hong, N. Nishii, K. Sonogashira, and N. Hagihara, *J. Chem. Soc., Chem. Commun.*, 993 (1972); T. Yamamoto and A. R. Garber, *ibid.*, 354 (1974); H. Ueda, Y. Kai, N. Yasuoka, and N. Kasai, *Bull. Chem. Soc. Jpn.*, **50**, 2250 (1977).
- F. N. Tebbe, G. W. Parshall, and G. S. Reddy, *J. Am. Chem. Soc.*, **100**, 3611 (1978).
- Preliminary note: R. A. Andersen, R. A. Jones, G. Wilkinson, K. M. A. Malik, and M. B. Hursthouse, *J. Chem. Soc., Chem. Commun.*, 865 (1977).
- R. A. Andersen, R. A. Jones, G. Wilkinson, K. M. A. Malik, and M. B. Hursthouse, *J. Chem. Soc., Chem. Commun.*, 283 (1977); R. A. Andersen, R. A. Jones, and G. Wilkinson, *J. Chem. Soc., Dalton Trans.*, 446 (1978).
- A. Spencer and G. Wilkinson, *J. Chem. Soc., Dalton Trans.*, 1570 (1972).
- K. A. Raspin, *J. Chem. Soc. A*, 461 (1969).
- N. W. Alcock and K. A. Raspin, *J. Chem. Soc. A*, 2108 (1968).
- G. Chioccola, J. J. Daly, and J. K. Nicholson, *Angew. Chem., Int. Ed. Engl.*, **7**, 131 (1968).
- F. A. Cotton and J. M. Troup, *J. Chem. Soc., Dalton Trans.*, 800 (1974).
- A. F. Masters, K. Mertis, J. F. Gibson, and G. Wilkinson, *Nouveau J. Chim.*, **1**, 389 (1977).
- J. Holton, M. F. Lappert, D. G. H. Ballard, R. Pearce, J. L. Atwood, and W. E. Hunter, *J. Chem. Soc., Chem. Commun.*, 480 (1976).
- P. G. Edwards, K. Mertis, and G. Wilkinson, *J. Chem. Soc., Dalton Trans.*, in press.
- R. B. Calvert and J. R. Shapley, *J. Am. Chem. Soc.*, **100**, 7726 (1978). See also R. B. Calvert and J. R. Shapley, A. J. Schultz, J. M. Williams, S. L. Suib, and G. D. Stucky, *ibid.*, **100**, 6240 (1978). The significant difference in the ^1H NMR chemical shifts for the μ - CH_3 and μ - CH_2D groups ($\Delta = 0.20 \text{ ppm}$ at 35°C in CD_3NO_2) is much larger than that expected for a simple isotope effect and suggests a C–H \cdots Ru interaction in solution, possibly similar to that described by Shapley for " $^1\text{Os}_3(\text{CO})_{10}\text{CH}_2\text{D}_2$ ". Variable-temperature ^1H NMR studies show that Δ is only slightly temperature dependent (in CD_3NO_2 at 80°C , $\Delta = 0.15 \text{ ppm}$; at -90°C in CD_2Cl_2 , $\Delta = 0.25 \text{ ppm}$), indicating only a slight interaction of the methyl proton(s) with the metal. However, there is no further evidence for this interaction in the solid state. We have considered a suggestion by Shapley that the methyl group might be bound by a C–H \cdots Ru bridge to each metal atom leading to a disordered, off-center situation, but cannot reconcile this with the normal geometrical requirement of a bridging methyl group. If we do disregard the idea of a bridge made up from a normal Ru– CH_3 σ link to one metal atom and a C–H \cdots Ru link to the other (see text), then the sp^3 hybrid orbital of the CH_3 group used for the 3c–2e "Ru–C–Ru" bridge would be expected to lie in a plane perpendicular to and bisecting the Ru–Ru vector. If we then tilt the CH_3 group to bring two of the hydrogen atoms closer to the metal atoms, then this lobe must move out of the Ru–C–Ru plane. This would result in considerably diminished overlap, which we feel is unlikely. A neutron diffraction study could be useful and we are hoping to organize this.
- See, for example, *Spec. Period. Rep.: Mol. Struct. Diff. Methods*, **4**, 328–340 (1976).
- R. Manson, K. M. Thomas, D. F. Gill, and B. L. Shaw, *J. Organomet. Chem.*, **40**, C67 (1972).
- L. Ricard, C. Martin, R. Wiest, and R. Weiss, *Inorg. Chem.*, **14**, 2300 (1975); B. Spivack, Z. Dori, and E. I. Steifel, *Inorg. Nucl. Chem. Lett.*, **11**, 501 (1975).
- G. M. Sheldrick, SHELX Crystallographic Calculation Program, University of Cambridge, 1976.
- In order to test the possibility that the space group was Pn , we refined a model in this space group, in which the asymmetric unit was one complete molecule, tilt slightly off the line of the twofold axis in $P2_1/n$, but the refinement was very unstable and the split C(2) peak always persisted, astride the position of the twofold axis.
- D. T. Cromer and J. B. Mann, *Acta Crystallogr., Sect. A*, **24**, 321 (1968).
- R. F. Stewart, E. R. Davidson, and W. T. Simpson, *J. Chem. Phys.*, **42**, 3175 (1965).
- D. T. Cromer and D. Liberman, *J. Chem. Phys.*, **53**, 1891 (1970).
- C. K. Johnson, ORTEP, Report ORNL-3794, Oak Ridge National Laboratory, Oak Ridge, Tenn., 1965.
- W. D. S. Motherwell, PLUTO, University of Cambridge, England.